Color superconducting quark matter core in the third family of compact stars

Sarmistha Banik and Debades Bandyopadhyay
Saha Institute of Nuclear Physics, 1/AF Bidhannagar, Kolkata 700 064, India

Abstract

We investigate first order phase transitions from β-equilibrated hadronic matter to color flavor locked quark matter in compact star interior. The hadronic phase including hyperons and Bose-Einstein condensate of K^- mesons is described by the relativistic field theoretical model with density dependent meson-baryon couplings. The early appearance of hyperons and/or Bose-Einstein condensate of K^- mesons delays the onset of phase transition to higher density. In the presence of hyperons and/or K^- condensate, the overall equations of state become softer resulting in smaller maximum masses than the cases without hyperons and K^- condensate. We find that the maximum mass neutron stars may contain a mixed phase core of hyperons, K^- condensate and color superconducting quark matter. Depending on the parameter space, we also observe that there is a stable branch of superdense stars called the third family branch beyond the neutron star branch. Compact stars in the third family branch may contain pure color superconducting core and have radii smaller than those of the neutron star branch. Our results are compared with the recent observations on RX J185635-3754 and the recently measured mass-radius relationship by X-ray Multi Mirror-Newton Observatory.

I. INTRODUCTION

The theoretical investigation of mass-radius relationship of compact stars is important because those could be directly compared with measured masses and radii from various observations. Consequently, the composition and equation of state (EoS) of dense matter in neutron star interior might be probed. Recently, a lot of interest has been generated about an isolated neutron star (INS) known as RX J185635-3754 [1]. Several interesting features of this INS have emerged from various observations by Chandra X-ray observatory and Hubble Space Telescope (HST). It is one of the closest isolated neutron stars to our Sun. It provides a great opportunity to measure its radius and put important constraints on the EoS of dense matter in its core because of its relative brightness, isolated nature and above all a thermal spectrum from X-ray to optical wave lengths. Already, one group who has analysed the Chandra data using a featureless blackbody spectrum, has claimed its radius is ~ 8 km or less [2]. This implies a very soft EoS including exotic forms of matter. And their prediction is the compact star might be a quark star [2]. Alternatively, the Chandra data have been

interpreted using a neutron star model where the gaseous outer layers of the neutron star turn into a solid due to a phase transition and this model gives an apparent radius $\sim 10-12$ km [3]. On the other hand, the analysis of HST data on that compact star indicated a radius R=11.4 ± 2 km and a mass M=$1.7 \pm 0.4 M_{solar}$ which may be explained by many EoS including hyperons and antikaon condensate [4]. Recently three strong spectral lines in the spectra of 28 bursts of low mass X-ray binary EXO0748-676 have been observed by X-ray Multi Mirror-Newton Observatory. The estimated gravitational red shift from those lines is $z = 0.35$ [5]. This provides us with many important informations about the structure of compact star because the gravitational redshift depends on the mass-radius ratio of a compact star.

The composition and structure of compact stars depend on the nature of strong interaction. Neutron star matter encompasses a wide range of densities- the density of iron nucleus at the surface to several times normal nuclear matter density in the core. Different phases of exotic matter with large strangeness fraction such as hyperon matter [6], Bose-Einstein condensates of strange mesons [7–14] and quark matter [6,8,15,16] may occur in neutron star interior. It was extensively investigated how the appearance of various forms of exotic matter influences the EoS and mass-radius relationship of compact stars. It is now well understood that each exotic component of dense matter makes the EoS soft. It was found in theoretical investigations [17] that a soft EoS generally gave rise to a compact star with smaller maximum mass and radius than those of a stiffer EoS.

A transition from hadronic matter to deconfined strange quark matter is a possibility in neutron star interior. In earlier investigations, the quark phase was described by the MIT bag model [6,15] in the hadron-quark phase transition. The recent development in dense matter physics points to the fact that the quark matter may be a color superconductor [18–24]. In this case, quarks near their Fermi surfaces form Cooper pairs because quark-quark interaction is attractive in the antisymmetric color channel. The formation of diquark condensates breaks the color gauge symmetry. It was shown that at very high density quarks with all three flavors and all three colors might pair up so as to produce an energetically favored state called the color-flavor-locked (CFL) phase [25]. The color neutrality constraint is to be imposed in the CFL quark matter because a macroscopic chunk of quark matter must be color singlet [26,27]. Consequently, the CFL quark matter is charge neutral. Color and charge neutrality in the CFL quark matter require a non-zero value for the color chemical potential and electron chemical potential $\mu_e = 0$ respectively [26,27]. As the CFL condensate breaks chiral symmetry, the lightest degrees of freedom in this phase are Nambu-Goldstone bosons [25,28,29]. It was shown by various groups how the symmetric CFL phase behaves under stresses such as non-zero strange quark mass and electron chemical potential [28,29]. The CFL phase could relax under those stresses forming meson condensation. One such possibility is K^0 condensation in the charge neutral CFL quark matter [28].

Recently, nuclear-CFL quark matter phase transition [30] and its impact on the structure of compact stars have been studied [31]. Also, the structure of compact stars including pure CFL quark matter has been studied by others [32]. Along with CFL quark matter, hyperons and K^- condensate could exist in compact star interior. Many interesting things may happen if one form of exotic matter sets in before the other. The early appearance of hyperons was found to delay the hadron-unpaired quark matter phase transition or vice-versa [8]. Similar effects of hyperons on the threshold of K^- condensation in hadronic matter was observed

by various groups [8,11–14]. Now the question is what could happen to nuclear-CFL quark matter phase transition if hyperons and K^- condensate appear in compact star matter. So far no calculation of compact stars involving color superconducting quark matter, hyperons and K^- condensate has been performed. In this paper, we investigate how the formation of hyperons and antikaon condensate in the hadronic matter influences the phase transition from hadronic matter to the CFL quark matter including K^0 condensate and the structure of compact stars. The paper is organised in the following way. In Sec. II, we describe the DDRH model for hadronic phase and also the CFL quark matter. Results of our calculation are explained in Sec. III. And Sec. IV provides a summary and conclusions.

II. FORMALISM

Here, we discuss a phase transition from hadronic matter to the CFL quark matter in compact stars. The β-equilibrated and charge neutral bulk hadronic phase is described within the framework of a Density Dependent Relativistic Hadron (DDRH) model [14,33–36]. In the DDRH model, many body correlations are taken into account by density dependent meson-baryon couplings. The hadronic phase is composed of all species of the baryon octet, (anti)kaons, electrons and muons. Therefore, the total Lagrangian density in the hadronic phase is written as $\mathcal{L} = \mathcal{L}_B + \mathcal{L}_K + \mathcal{L}_l$. In the DDRH model, baryon-baryon interaction is given by the Lagrangian density ($\mathcal{L}_B$) [34],

$$\begin{aligned}\mathcal{L}_B = \sum_B \bar{\Psi}_B \Big(i\gamma_\mu \partial^\mu - m_B + g_{\sigma B}\sigma - g_{\omega B}\gamma_\mu \omega^\mu - \frac{1}{2} g_{\rho B}\gamma_\mu \boldsymbol{\tau}_B \cdot \boldsymbol{\rho}^\mu + \frac{1}{2} g_{\delta B} \boldsymbol{\tau}_B \cdot \boldsymbol{\delta} \Big) \Psi_B \\ + \frac{1}{2}\left(\partial_\mu \sigma \partial^\mu \sigma - m_\sigma^2 \sigma^2 \right) + \frac{1}{2}\left(\partial_\mu \delta \partial^\mu \delta - m_\delta^2 \delta^2 \right) - \frac{1}{4}\omega_{\mu\nu}\omega^{\mu\nu} \\ + \frac{1}{2} m_\omega^2 \omega_\mu \omega^\mu - \frac{1}{4}\boldsymbol{\rho}_{\mu\nu} \cdot \boldsymbol{\rho}^{\mu\nu} + \frac{1}{2} m_\rho^2 \boldsymbol{\rho}_\mu \cdot \boldsymbol{\rho}^\mu . \end{aligned} \tag{1}$$

The Lagrangian density for (anti)kaon condensation in the minimal coupling scheme [10,14] is

$$\mathcal{L}_K = D_\mu^* \bar{K} D^\mu K - m_K^{*2} \bar{K} K \ , \tag{2}$$

where the covariant derivative $D_\mu = \partial_\mu + i g_{\omega K}\omega_\mu + i g_{\rho K} \boldsymbol{\tau}_K \cdot \boldsymbol{\rho}_\mu/2$ and the effective mass of (anti)kaons $m_K^* = m_K - g_{\sigma K}\sigma + \frac{1}{2} g_{\delta K}\delta$. Unlike meson-baryon couplings, meson-(anti)kaon couplings are density-independent here. The threshold condition of K^- condensation is $\omega_{K^-} = \mu_e$, where ω_{K^-} is the in-medium energy of K^- mesons for s-wave condensation [14].

The Lagrangian density for leptons is

$$\mathcal{L}_l = \sum_l \bar{\psi}_l \left(i\gamma_\mu \partial^\mu - m_l \right) \psi_l \ , \tag{3}$$

where ψ_l ($l \equiv e, \mu$) is lepton spinor.

The charge neutrality condition in the bulk hadronic phase is

$$Q^h = \sum_b q_b n_b^h - n_{K^-} - n_e - n_\mu = 0, \tag{4}$$

where q_b and n_b^h are electric charge and the number density of baryon b in the pure hadronic phase, respectively and n_{K^-}, n_e and n_μ are number densities of K^-, electrons and muons respectively. The energy density (ε^h) and the pressure (P^h) in the hadronic phase are given by Ref. [14].

The pure CFL quark matter is composed of paired quarks of all flavors and colors and neutral kaons which are Goldstone bosons arising due to the breaking of chiral symmetry in the CFL phase. The thermodynamic potential for electric and color charge neutral CFL quark matter to order Δ^2 is given by [25,30,31]

$$\Omega^q_{CFL} = \frac{6}{\pi^2}\int_0^\nu p^2(p-\mu)dp + \frac{3}{\pi^2}\int_0^\nu p^2(\sqrt{p^2+m_s^2}-\mu)dp - \frac{3\Delta^2\mu^2}{\pi^2} + B \ , \tag{5}$$

where Δ is the color superconducting gap and B is the bag contribution. The first two terms of Eq. (5) give the thermodynamic potential of (fictional) unpaired quark matter in which all quarks that are going to pair have a common Fermi momentum ν which minimizes the thermodynamic potential of the fictional unpaired quark matter [25,30,31]. The third term is the contribution of the CFL condensate to Ω^q_{CFL}. The common Fermi momentum is

$$\nu = 2\mu - \sqrt{\mu^2 + \frac{m_s^2}{3}} \ , \tag{6}$$

where μ is the average quark chemical potential and m_s is the strange quark mass. Studying the pairing ansatz in the CFL phase, it was shown by various authors [27] that

$$n_u = n_r, \qquad n_d = n_g \qquad \text{and} \qquad n_s = n_b \ , \tag{7}$$

where n_r, n_g, n_b and n_u, n_d, n_s are color and flavor number densities respectively. It follows from the above relation that color neutrality automatically enforces electric charge neutrality in the CFL phase. The quark number densities are $n_u = n_d = n_s = (\nu^3 + 2\Delta^2\mu)/\pi^2$. As the color neutral CFL quark matter is electric charge neutral, the corresponding electric charge chemical potential is $\mu_e = 0$. Similarly, the color chemical potential corresponding to color charge T_3 is $\mu_3 = 0$. However, the color chemical potential for color charge T_8 is $\mu_8 \neq 0$ to maintain color charge neutrality in the CFL phase [26,27].

The thermodynamic potential ($\Omega^{K^0}_{CFL}$) due to K^0 condensate is given by Ref. [28]. The pressure in the CFL phase including K^0 condensate is given by $P^q = -\Omega^q_{CFL} - \Omega^{K^0}_{CFL}$. The energy density ($\epsilon^q$) in the CFL phase is obtained from the Gibbs-Duhem relation [37].

We now describe the mixed phase of the above mentioned two phases because the phase transition from hadronic to the CFL quark matter is a first order phase transition. Earlier the mixed phase of hadronic and unpaired quark matter was studied by various authors [6,16,38]. In that case, baryon number and electric charge were two conserved charges in individual bulk phase. Glendenning argued conserved charges may be shared by two phases in equilibrium in the coexistence phase and the mixed phase is to be determined by Gibbs conditions along with global baryon and electric charge conservation laws [38]. It was found that the net positive charge of the hadronic phase was neutralised by the net negative charge of the unpaired quark matter in the mixed phase. Unlike unpaired quark matter, electric charge is not present in the CFL quark matter. And baryon and color charge are conserved quantities in the CFL phase. Recently, the mixed phase of nuclear and CFL quark matter

including Goldstone bosons π^- or K^- was constructed using Glendenning's prescription [30,31]. It was shown there that K^- or π^- condensate was formed at the cost of electrons of the hadronic phase and made the CFL phase negatively charged in the mixed phase. As color charge in the bulk hadronic phase and electric charge in the bulk CFL phase can not be present, we relax the global conservation laws of Glendenning [38] and consider only local electric charge neutrality in the hadronic phase and local color charge neutrality in the CFL phase. Here the mixed phase is determined by Gibbs phase rules and the global conservation law for baryon number. The Gibbs conditions read

$$P^h = P^q \ , \tag{8}$$

$$\mu_n = 3\mu \ , \tag{9}$$

where μ_n and μ are neutron and quark chemical potential. The global baryon number conservation law is imposed through the relation

$$n_b = (1-\chi)n_b^h + \chi n_b^q \ , \tag{10}$$

where χ is the volume fraction of the CFL phase in the mixed phase and n_b^h and n_b^q are baryon densities in the hadronic and CFL phase respectively. The total energy density in the mixed phase is

$$\epsilon = (1-\chi)\epsilon^h + \chi\epsilon^q \ . \tag{11}$$

III. RESULTS AND DISCUSSIONS

In the DDRH model, the dependence of meson-nucleon vertices on total baryon density is obtained from microscopic Dirac-Brueckner calculations of symmetric and asymmetric matter using Groningen nucleon-nucleon potential [39–41]. We adopt a suitable parameterisation for density dependent couplings as was given by Ref. [33]. The density dependent meson-nucleon couplings at saturation density are listed in Table I of Ref. [14]. The saturation properties calculated using these couplings are binding energy E/A=-15.6 MeV, saturation density $n_0 = 0.18fm^{-3}$, symmetry energy coefficient $a_{sym} = 26.1$ MeV and incompressibility K = 282 MeV [14].

The density dependence of meson-hyperon vertices are obtained from density dependent meson-nucleon couplings using hypernuclear data [9] and scaling law [42]. The ratio of meson-hyperon coupling to meson-nucleon coupling for Groningen potential is given by Table II of Ref. [14]. Similarly, we employ the density independent meson-(anti)kaon couplings of Ref. [14] in our calculation.

Now we report results of our calculation. We have performed calculations for compact star matter allowing first order phase transition from i) nuclear to CFL quark matter (np$\rightarrow$ CFL+K^0), ii) nuclear+K^-condensate to CFL quark matter (np$K^-\rightarrow$ CFL+K^0), iii) hyperonic matter to CFL quark matter (np$\Lambda\Xi\rightarrow$ CFL+K^0), and iv) hadronic matter including hyperons and K^- condensate to CFL quark matter (np$\Lambda\Xi K^-\rightarrow$ CFL+K^0). In this calculation, we have neglected the density dependence of strange quark mass (m_s), color superconducting gap (Δ) and bag constant ($B^{1/4}$).

First we discuss np$\rightarrow$ CFL+K^0 (denoted hereafter by NQ) matter phase transition for different values of gap and strange quark mass whereas the bag constant is fixed at $B^{1/4} = 180$ MeV. We also show the results of nuclear to unpaired ($\Delta = 0$) quark matter phase transition. Nuclear matter is composed of neutrons, protons, electrons and muons whereas the CFL phase contains paired quarks and K^0 condensate. For nuclear to unpaired quark matter phase transition, we have imposed both global baryon and electric charge conservation in the mixed phase. On the other hand, we have global baryon number conservation and local color and electric charge neutrality in the mixed phase of nuclear-CFL phase transition. The lower and upper boundary of the mixed phase for $\Delta = 0$, 57 and 100 MeV and $m_s = 150$ and 200 MeV and $B^{1/4} = 180$ MeV are recorded in Table I. The onset of phase transition is at $u_l = n_l/n_0$ and the pure CFL phase begins at $u_u = n_u/n_0$. Here we note that the phase transition to quark matter is delayed to higher densities for a larger value of m_s. On the other hand, the phase transition occurs earlier for case $\Delta = 100$ MeV than that of case $\Delta = 0$ and 57 MeV irrespective of strange quark mass. We also note that the extent of the mixed phase involving unpaired quark matter is the largest among all the cases studied here. The average quark chemical potential at the onset of the phase transition is shown in Table I. We find that the CFL phase is energetically favoured over unpaired quark matter because $\Delta > m_s^2/4\mu$ is satisfied [26].

Pressure versus energy density and gravitational mass against central energy density for compact stars with NQ matter and different values of gap ($\Delta = 0, 57$ and 100 MeV), $m_s = 150$ and 200 MeV and $B^{1/4} = 180$ MeV are exhibited in Fig. 1 and Fig. 2 respectively. The static structures of spherically symmetric neutron stars calculated using Tolman-Oppenheimer-Volkoff (TOV) equations and the equations of state of Fig. 1, are presented in Fig. 2. We adopt Negele and Vautherin [43] and Baym-Pethick-Sutherland [44] equations of state to describe nuclear matter at very low density. The maximum neutron star masses (M/M_{solar}) and their corresponding central densities ($u_{cent} = n_{cent}/n_0$) are listed in Table I. For unpaired quark matter and paired quark matter with $\Delta = 57$ MeV, the overall EoS with $m_s = 200$ MeV is stiffer than that of $m_s = 150$ MeV. Consequently, the compact star in the former case has a larger maximum mass than that of the latter case. The effect of m_s is pronounced for unpaired quark matter. However, for $\Delta = 100$ MeV and different values of m_s there is no significant change in the EoS and maximum star masses. Again, we find the maximum masses for $\Delta = 57$ MeV are reduced compared with those for $\Delta = 100$ MeV because the EoS in the latter case is stiffer. From Table I, it is observed that compact stars have pure CFL quark matter core for $\Delta = 100$ MeV whereas compact stars, in other cases, contain a mixed phase core of nuclear and unpaired or CFL quark matter. We note that K^0 condensate in the CFL phase does not contribute significantly in the energy density and pressure. Recently, Alford and Reddy [31] also investigated the influence of m_s and Δ on the EoS and structure of compact stars in nuclear-CFL quark matter phase transition using different models for the hadronic phase. Our results for stars including NQ matter are in qualitative agreement with their findings. In our calculation, we do not consider the variation of bag constant on nuclear-CFL quark matter phase transition. But we expect similar qualitative feature as it was observed for the phase transition involving unpaired quark matter. It is worth mentioning here that a larger value of bag constant makes the EoS of unpaired quark matter soft delaying the phase transition to higher density [8].

In earlier investigations, it was shown that exotic components of matter such as hy-

perons [6], Bose-Einstein condensate of K^- mesons [11–14] and quarks [8] could appear in β-equilibrated and electric charge neutral matter around (2-4)n_0. It was also studied how hyperons delayed the onset of antikaon condensation [11–14] and the phase transition to unpaired quark matter [8] to higher density. With the appearance of each exotic phase in dense matter, the EoS becomes softer. Here we perform calculation involving hyperons, antikaon condensate and quarks and examine how exotic phases of matter compete with each other in compact star interior. Also, we explore whether there is any window in the parameter space for which all three exotic components of matter may coexist in the core of compact stars and its implication on their structures.

In Table II, we show the mixed phase boundaries for compact star matter that undergoes first order phase transition from npΛΞ→ CFL+K^0 (denoted by NHQ), npK^-→ CFL+K^0 (N$\bar{K}$Q) and npΛΞK^-→ CFL+K^0 (NH$\bar{K}$Q). These results are obtained for strange quark mass $m_s = 150$ MeV. The early appearance of hyperons in NHQ star matter at $1.99n_0$ gives rise to a softer EoS delaying the phase transition to CFL quark matter to higher densities for all values of bag constants and gap as are shown in Table II. On the other hand, for N$\bar{K}$Q matter with $B^{1/4} = 180$ MeV and antikaon optical potential depth $U_{\bar{K}} = -180$ MeV, the onset of K^- condensation produces a softer EoS postponing the CFL phase with $\Delta = 30$ MeV to higher density and the reverse happens for the CFL phase with $\Delta = 57$ MeV. In the calculation of NH$\bar{K}$Q matter using $B^{1/4} = 180(185)$ MeV, $\Delta = 30(57)$ MeV and $U_{\bar{K}} = -180(-160)$ MeV, hyperons and K^- condensate appear before the phase transition to the CFL phase. In the other case with $B^{1/4} = 180$ MeV, $\Delta = 57$ MeV and $U_{\bar{K}} = -180$ MeV, K^- condensate appear in the mixed phase. We also perform calculation for NHQ, N$\bar{K}$Q and NH$\bar{K}$Q matter using parameters $B^{1/4} = 180$ MeV, $\Delta = 100$ MeV $m_s = 150$ MeV and $U_{\bar{K}} = -180$ MeV. For all cases, we note that the early onset of CFL phase at $1.43n_0$ forbids hyperons and/or K^- condensate to appear in compact star matter. In the following two paragraphs, we discuss the compositions of compact star matter and how exotic phases of dense matter compete with each other.

The composition of β-equilibrated NHQ matter relevant to compact stars is displayed in Fig. 3. The hadronic phase is composed of n, p, Λ, Ξ and leptons. On the other hand, we have included the contribution of Goldstone boson K^0 in the CFL phase. Here, we take bag constant $B^{1/4} = 180$ MeV, $m_s = 150$ MeV and $\Delta = 57$ MeV to describe the CFL quark matter. The charge neutrality in the hadronic phase is maintained by protons, electrons and muons. We observe that Λ hyperons appear at $1.99n_0$, where $n_0 = 0.18\ fm^{-3}$. The phase transition from hadronic to CFL quark matter sets in at $2.27n_0$. The mixed phase is over at $3.97n_0$. It is noted here that negatively charged Ξ hyperons appear just before the onset of mixed phase at $2.26n_0$. With the appearance of Ξ^- hyperons, the density of electrons drops fast. Also, neutral K^0 condensation appears with the onset of CFL phase and it rises rapidly.

Along with hyperons, we also investigate the role of K^- condensation in the hadronic phase on the composition of NH$\bar{K}$Q star matter. In a recent calculation using DDRH model, it has been shown that K^- condensation in hadronic matter is a second order phase transition [14]. In Fig. 4 we exhibit the particle abundances in β-equilibrated NH$\bar{K}$Q matter. The antikaon optical potential used for this calculation is $U_{\bar{K}}(n_0) = -180$ MeV and bag constant, strange quark mass and gap are 180, 150 and 57 MeV respectively. Here we find that the mixed phase begins at the same density point i.e. $2.27n_0$ as it is noted in

Fig. 3. Before the onset of K^- condensate, the charge neutrality is maintained by protons and leptons. The condensation of K^- mesons occurs in the mixed phase at $2.68n_0$. As soon as K^- condensate appears, it rapidly replaces electrons and muons and grows fast. Consequently, proton density increases. Also, we observe that negatively charged Ξ hyperon disappears almost as soon as it appears. There is no influence of K^- condensate on the extent of the mixed phase because K^- condensate appears in the mixed phase.

Equations of state (pressure versus energy density) for β-equilibrated and charge neutral NQ and NHQ compact star matter are plotted in Fig. 5. The curves correspond to calculations for $m_s = 150$ MeV and different values of bag constant and gap. The dashed line stands for the EoS of NQ matter whereas the other lines represent those of NHQ matter for different parameter sets. For $B^{1/4} = 180$ MeV and $\Delta = 57$ MeV, the EoS for NHQ matter is slightly softer compared with the corresponding EoS for NQ matter. As the bag constant is increased keeping the gap fixed, we find the corresponding equations of state become stiffer. The stiffest EoS among all cases considered here corresponds to the EoS for NHQ matter with $\Delta = 30$ MeV.

The maximum neutron star masses (M_{max}/M_{solar}) and their central densities ($u_{cent} = n_{cent}/n_0$) calculated with the above mentioned equations of state including NQ and NHQ matter are listed in Table I and Table II. The static neutron star sequences representing the stellar masses M/M_{solar} and the corresponding central energy densities (ε_c) for different values of bag constant and gap are shown in Fig. 6. The closed circle on each curve denotes the maximum mass star. For $B^{1/4} = 180$ MeV and $\Delta = 57$ MeV, the maximum mass of NQ star is $1.500M_{solar}$ corresponding to central energy density 717.46 MeV/fm^3, whereas that of NHQ star is $1.477M_{solar}$ corresponding to $\varepsilon_c = 717.47$ MeV/fm^3. The maximum mass of the star including hyperons is smaller than that of the star with NQ matter because the EoS is softer in former case. The maximum masses of compact stars increase as we increase the bag constant or decrease the gap. This is evident from Fig. 6 and Table II. We also note from Table II that the central densities corresponding to maximum masses of neutron stars including NHQ matter fall in the mixed phase. Consequently the maximum mass neutron stars contain a hyperon-CFL quark mixed phase core. For each of the bottom three curves in Fig. 6, we find an unstable region followed by a stable sequence of superdense stars beyond the neutron star branch. The stable branch of superdense stars beyond the neutron star branch is called the third family branch [13,16,45–48]. It was earlier shown by various authors that the compact stars in the third family branch had different compositions and smaller radii than those of the neutron star branch. In this calculation, the superdense stars in the third family branch may contain a pure CFL quark matter core because those stars appear after the mixed phase is over.

We also calculate the EoS and structure of compact stars in the phase transition from hadronic matter including both hyperons and K^- condensate to CFL quark matter. Equations of state and compact star mass sequences calculated with N$\bar{K}$Q and NH$\bar{K}$Q matter are plotted in Fig. 7 and Fig. 8 respectively for various parameter sets. The maximum neutron star masses with their central densities are given by Table II. The dashed line corresponds to N$\bar{K}$Q matter whereas the other curves represent NH$\bar{K}$Q matter in both the figures. In Fig. 8 we find that the static neutron star sequence for NH$\bar{K}$Q matter with $B^{1/4} = 180$ MeV, $\Delta = 57$ MeV, $m_s = 150$ MeV and $U_{\bar{K}}(n_0) = -180$ MeV has a lower maximum mass $1.464M_{solar}$ corresponding to central energy density ε_c =690.19 MeV/fm^3

than the corresponding N$\bar{K}$Q star of $1.503M_{solar}$ corresponding to central energy density ε_c =689.59 MeV/fm^3. This may be attributed to the fact that the EoS in the former case is softer than that of the latter case as it is evident from Fig. 7. Here it is interesting to note that the maximum mass neutron star including NH$\bar{K}$Q matter has a mixed phase core where hyperons, antikaon condensate and CFL quarks coexist. Similar situation occurs in NH$\bar{K}$Q star for $\Delta = 30$ MeV. From Fig. 8, we find third family solutions beyond neutron star branches in two cases. Here superdense stars in the third family also contain a pure CFL quark matter core. For the other case studied with $B^{1/4} = 185$ MeV, $\Delta = 57$ MeV, $m_s = 150$ MeV and $U_{\bar{K}}(n_0) = -160$ MeV, we obtain a stiffer EoS resulting in a larger maximum mass star $1.582M_{solar}$ corresponding to central energy density ε_c =803.32 MeV/fm^3.

We have also performed calculation for stars with NH$\bar{K}$Q matter using a larger strange quark mass $m_s = 200$ MeV, $B^{1/4} = 180$ MeV, $U_{\bar{K}} = -180$ MeV and different values of gap. For $\Delta = 30$ and 57 MeV, the phase transition does not begin even at density as high as $5.2n_0$ due to the softer EoS resulting from the early appearance of hyperons and K^- condensate. And the CFL phase does not occur in the corresponding maximum mass neutron star of 1.497 M_{solar} at central density $5.16n_0$. On the other hand, the CFL phase becomes stiffer in the calculation with $\Delta = 100$ MeV and the phase transition occurs at low density $1.76n_0$. Consequently, hyperons and K^- do not appear in the corresponding maximum mass star of 1.639 M_{solar} at central density $8.81n_0$.

The mass-radius relationship of compact stars with NQ, NHQ, N$\bar{K}$Q and NH$\bar{K}$Q matter for $B^{1/4} = 180$ MeV, $\Delta = 57$ MeV, $m_s = 150$ MeV and $U_{\bar{K}}(n_0) = -180$ MeV are shown in Fig. 9. The filled circles, squares and triangles correspond to maximum masses on the neutron star and third family branch. The maximum masses and radii of NQ stars (dotted line) in the neutron star (third family) branch are $1.500(1.506)M_{solar}$ and 12.37(10.15) km respectively. The presence of K^- condensate in N$\bar{K}$Q stars does not change maximum masses as it is evident from Table II. The maximum masses and their corresponding radii for NH$\bar{K}$Q stars (solid line) in the neutron star (third family) branch are $1.464(1.492)M_{solar}$ and 12.34(9.97) km whereas those for NHQ stars (dashed line) are $1.477(1.498)M_{solar}$ and 12.33(10.05) km respectively. Both the neutron star and third family branch have smaller masses in NH$\bar{K}$Q case than those in NHQ case because the EoS are softer in the former case. It is interesting to note that the radii in the third family branch are smaller than their counterparts in the neutron star branch. Also, the stars in the third family branch have different compositions than those of the neutron star branch. Recently, it has been predicted in a perturbative QCD calculation that the maximum mass and radius of the superdense star in the third family may be $\sim 1M\odot$ and 6 km respectively [48]. In Fig. 9 we also show the mass-radius relationship for NQ stars with $B^{1/4} = 180$ MeV, $\Delta = 100$ MeV and $m_s =$ 150 and 200 MeV. The maximum masses (radii) of compact stars for $m_s = 150$ and 200 MeV are 1.649 $M_\odot$ (9.48 km) and 1.639 $M_\odot$ (9.81 km) respectively. In both cases, no third family branch occurs.

From our investigation of compact stars with exotic forms of matter, it is observed that the thresholds of hyperons, antikaon condensation and CFL quark phase are sensitive to the hadronic EoS, bag constant, gap and strange quark mass. For parameters adopted in our calculation including CFL quark matter, maximum neutron star masses range from 1.464 to 1.649 M_{solar} (Table I and Table II). In the compact star with maximum mass 1.464 M_{solar}, all three exotic forms of matter are found to coexist whereas the star having a maximum

mass 1.649 M_{solar} is composed of nuclear+CFL quark matter and has a pure CFL quark matter core. Similar maximum neutron star masses were found in the calculations including only hyperons and antikaon condensate [12–14] and also in the calculation of nuclear-CFL quark matter phase transition [31].

Now we compare our results with the findings from various observations. It is argued that those equations of state which predict larger theoretically calculated maximum neutron star mass (M_{max}^{theo}) than the highest measured neutron star mass (M_{high}^{obs}), are acceptable [49]. So far highest accurately measured compact star mass is the Hulse Taylor pulsar mass which is 1.44 M_{solar} [50]. Maximum neutron star masses obtained in our calculation are found to be larger than the Hulse Taylor pulsar mass i.e. $M_{max}^{theo} > M_{high}^{obs}$ is satisfied by our calculation. Recent observations on an isolated neutron star RX J185635-3754 by HST and Chandra X-ray observatory and low mass X-ray binary EXO0748-676 by XMM-Newton observatory have poured in many interesting data. Walter and Lattimer analysed HST data from RX J185635-3754 using an atmospheric model [4] and predicted radius R = 11.4 ± 2 km and mass M = 1.7 ± 0.4 M_{solar}. This result is in agreement with the masses and radii of compact stars from our model calculation. However, we can not construct any star with radius ~ 8 km or less as predicted by Drake et al. [2] analysing Chandra data on the same star. Another possible explanation of Chandra data is given by Zane et al. [3] and it indicates an apparent radius $\sim 10 - 12$ km which is compatible with our soft EoS. On the other hand, Cottam et al. [5] obtained a M-R relationship curve measuring the gravitational red shift $z = 0.35$ of three strong spectral lines in X-ray bursts from EXO0748-676. From this observational M-R relationship, one finds a range of possible values for compact star mass 1.2-1.8 M_{solar} corresponding to 8-12 km radius. In Fig. 9 we plot the results of Cottam et al. [5]. We note that some of our results are consistent with the observational M-R relationship curve. It shows that there may be room for exotic forms of matter to coexist in compact stars. As the mass of EXO0748-676 is not known, nothing can be concluded with certainty about dense matter EoS. Further measurements of gravitational redshift and mass on other neutron stars could put stringent conditions on theoretical models for dense matter in compact stars.

IV. SUMMARY AND CONCLUSIONS

We have investigated first order phase transitions from hadronic matter including hyperons and antikaon condensate to color-flavor-locked quark matter including the condensate of Goldstone boson K^0. The DDRH model has been adopted here to describe the hadronic phase. This model takes into account many body correlations in hadronic phase by density dependent meson-baryon couplings. Density dependent meson-baryon couplings are obtained from microscopic Dirac-Brueckner calculations using Groningen nucleon-nucleon potential. In this calculation meson-(anti)kaon couplings are density independent. Here K^- condensation is found to be a second order phase transition. On the other hand, the CFL quark matter is described by the thermodynamic potential of Ref. [25]. The role of strange quark mass and color-superconducting gap on the nuclear-CFL+K^0 matter phase transition has been studied for a fixed value of bag constant $B^{1/4} = 180$ MeV. The phase transition is delayed to higher density for a larger value of m_s. On the other hand, the phase transition sets in earlier as the value of gap increases. Also, we have found the early appearance of hyperons and /or Bose-Einstein condensate of K^- mesons shifts the phase transition to

higher density.

Equations of state for nuclear matter-CFL+K^0 matter phase transition have been studied here for different values of m_s and Δ and for a fixed value of bag constant. For a fixed value of gap, the EoS becomes stiffer in case of a larger value of m_s resulting in larger maximum mass star. For a large value of gap such as $\Delta = 100$ MeV, we find that different values of strange quark mass have no impact on the EoS and the maximum masses of compact stars. Similarly, a smaller value of gap softens the EoS leading to a smaller maximum mass star. We have also constructed equations of state including hyperons and K^- condensate in the hadronic phase for different values of bag constant, gap, antikaon optical potential depth and strange quark mass. The EoS for NHQ, N$\bar{K}$Q and NH$\bar{K}$Q matter are softer than that of NQ matter. Consequently, the maximum star masses are smaller in the former cases. For all cases studied here, maximum mass neutron stars contain a mixed phase core of hadronic+CFL quark matter. There is a window in the parameter space for which all three exotic forms of dense matter i.e. hyperons, Bose-Einstein condensate of K^- mesons and CFL quark matter are found to coexist in maximum mass neutron stars. In our calculation with CFL quark matter, maximum masses of compact stars range from 1.464 to 1.649 M_{solar}. Our results are consistent with the Hulse Taylor pulsar mass and recent observations. It is worth mentioning here that we have obtained stable branches of superdense stars called third family branches beyond neutron star branches for certain combinations of parameters. Superdense stars in the third family branch contain a pure CFL quark matter core. The compact stars in the third family have smaller radii and different compositions than those of the neutron star branch.

In this calculation, we do not consider the density dependence of strange quark mass, gap and bag parameter. Therefore, it would be interesting to investigate how density dependent strange quark mass, gap and bag parameter in the Nambu-Jona-Lasinio model [27] modify our results.

Acknowledgements

D.B. is grateful to Prof. (Dr.) W. Greiner for the warm hospitality of the Institut für Theoretische Physik, Frankfurt Universität where a part of the work was completed and the Alexander von Humboldt Foundation for the support.

REFERENCES

[1] J.A. Pons, F.M. Walter, J.M. Lattimer, M. Prakash, R. Neuhäuser and P. An, Astrophys. J **564**, 981 (2002).
[2] J.J. Drake et al., Astrophysics J. **572**, 996 (2002).
[3] S. Zane, R. Turolla and J.J. Drake, astro-th/0302197.
[4] F.M. Walter and J.M. Lattimer, Astrophys. J **564**, 981 (2002).
[5] J. Cottam, F. Paerels and M. Mendez, Nature **420**, 51 (2002);
C. Miller, Nature **420**. 31
[6] N. K. Glendenning, Compact stars, (Springer, New York, 1997).
[7] D.B. Kaplan and A.E. Nelson, Phys. Lett. B **175**, 57 (1986);
A.E. Nelson and D.B. Kaplan, Phys. Lett. B **192**, 193 (1987).
[8] M. Prakash, I. Bombaci, M. Prakash, Paul J. Ellis, J. M. Lattimer and R. Knorren, Phys. Rep. **280**, 1 (1997).
[9] J. Schaffner and I.N. Mishustin, Phys. Rev. C **53**, 1416 (1996).
[10] N.K. Glendenning and J. Schaffner-Bielich, Phys. Rev. Lett. **81**, 4564 (1998).
[11] S. Pal, D. Bandyopadhyay and W. Greiner, Nucl. Phys. **A674**, 553 (2000).
[12] S. Banik and D. Bandyopadhyay, Phys. Rev. C **63**, 035802 (2001).
[13] S. Banik and D. Bandyopadhyay, Phys. Rev. C **64**, 055805 (2001).
[14] S. Banik and D. Bandyopadhyay, Phys. Rev. C **66**, 065801 (2002).
[15] E. Farhi and R.L. Jaffe, Phys. Rev. D **30**, 2379 (1984).
[16] K. Schertler, C. Greiner, J. Schaffner-Bielich and M.H. Thoma Nucl. Phys. **A677**, 463 (2000).
[17] J. M. Lattimer and M. Prakash, Astrophys. J **550**, 426 (2001) .
[18] B.C. Barrois, Nucl. Phys. **B129**, 390 (1977).
[19] S. Frautschi, Proceedings of workshop on hadronic matter at extreme density, Erice, 1978.
[20] D. Bailin and A. Love, Phys. Rep. **107**, 325 (1984).
[21] M. Alford, K. Rajagopal and F. Wilczek, Phys. Lett. B **422**, 247 (1998).
[22] R. Rapp, T. Schäfer, E.V. Shuryak and M. Velkovsky, Phys. Rev. Lett. **81**, 53 (1998).
[23] M. Alford, K. Rajagopal and F. Wilczek, Nucl. Phys. **B537**, 443 (1999).
[24] D.H. Rischke and R.D. Pisarski, nucl-th/0004016.
[25] K. Rajagopal and F. Wilczek, Handbook of QCD, Edited by M. Shifman (World Scientific, Singapore, 2001).
[26] M. Alford and K. Rajagopal, JHEP **06**, 031 (2002).
[27] A. Steiner, S. Reddy and M. Prakash, Phys. Rev. D **66**, 094007 (2002).
[28] D.B. Kaplan and S. Reddy, Phys. Rev. D **65**, 054042 (2001).
[29] P.F. Bedaque and T. Schäfer, Nucl. Phys. **A677**, 802 (2002).
[30] M. Alford, K. Rajagopal, S. Reddy and F. Wilczek, Phys. Rev. D **64**, 074017 (2001).
[31] M. Alford and S. Reddy, nucl-th/0211046.
[32] G. Lugones and J. E. Horvath, astro-ph/0211638.
[33] F. Hofmann, C.M. Keil and H. Lenske, Phys. Rev. C **64**, 034314 (2001).
[34] F. Hofmann, C.M. Keil and H. Lenske, Phys. Rev. C **64**, 025804 (2001).
[35] C. Fuchs, H. Lenske and H.H. Wolter, Phys. Rev. C **52**, 3043 (1995).
[36] H. Lenske and C. Fuchs, Phys. Lett. B **345**, 355 (1995).
[37] J. Madsen, Phys. Rev. Lett. **87**, 172003 (2001).

[38] N.K. Glendenning, Phys. Rev. D **46**, 1274 (1992).
[39] F. de Jong and H. Lenske, Phys. Rev. C **57**, 3099 (1998).
[40] F. de Jong and H. Lenske, Phys. Rev. C **58**, 890 (1998).
[41] R. Malfliet, Prog. Part. Nucl. Phys. **21**, 207 (1988).
[42] C.M. Keil, F. Hofmann and H. Lenske, Phys. Rev. C **61**, 064309 (2001).
[43] J.W. Negele and D. Vautherin, Nucl. Phys. **A207**, 298 (1974).
[44] G. Baym, C.J. Pethick and P. Sutherland, Astrophys. J. **170**, 299 (1971).
[45] U.H. Gerlach, Phys. Rev. **172**, 1325 (1968).
[46] N. K. Glendenning and C. Kettner, Astron. Astrophys. **353**, L9 (2000).
[47] J. Schaffner-Bielich, M. Hanauske, H. Stöcker and W. Greiner, Phys. Rev. Lett. **89**, 171101 (2002).
[48] E.S. Fraga, R.D. Pisarski and J. Schaffner-Bielich, Phys. Rev. D **63**, 121702 (2001); Nucl. Phys. **A702**, 217 (2002).
[49] P. Haensel, astro-th/0301073.
[50] J.M. Weisberg and J.H. Taylor, Phys. Rev. Lett. **52**, 1348 (1984).

TABLES

TABLE I. Lower(u_l) and upper(u_u) boundary of the mixed phase in nuclear-CFL phase transition for different values of gap $\Delta = 0$ (unpaired quark matter), 57, 100 MeV and strange quark mass $m_s = 150$ and 200 MeV for a given value of bag constant $B^{1/4} = 180$ MeV. Here $u = n_B/n_0$ and saturation density is $n_0 = 0.18fm^{-3}$. Average quark chemical potential at the onset of phase transition is also given here. The maximum neutron star masses M_{max}/M_{solar} and their corresponding central densities u_{cent}=n_{cent}/n_0 are shown below.

$B^{\frac{1}{4}}$ (MeV)	m_s (MeV)	Δ (MeV)	μ (MeV)	u_l	u_u	u_{cent}	$\frac{M_{max}}{M_{solar}}$
180	150	0	360.03	1.90	5.33	4.77	1.615
180	”	57	374.65	2.14	3.97	3.97	1.500
180	”	100	336.07	1.43	3.09	9.13	1.649
180	200	0	375.06	2.14	5.77	4.51	1.763
180	”	57	480.74	3.57	4.61	4.61	1.600
180	”	100	352.08	1.76	3.36	8.81	1.639

TABLE II. The maximum neutron star masses M_{max}/M_{solar} and their corresponding central densities u_{cent}=n_{cent}/n_0 with different compositions in a first order hadronic to CFL quark matter phase transition. The lower (u_l) and upper(u_u) boundary of the mixed phase and the threshold density of K^- condensation in hadronic phase $u_{th}^{K^-}$, where $u = n_B/n_0$, for antikaon optical potential depth $U_{\bar{K}}(n_0)$ MeV at saturation density $n_0 = 0.18fm^{-3}$ are given for various values of bag constant $B^{1/4}$ and gap Δ and strange quark mass $m_s = 150$ MeV.

	$B^{\frac{1}{4}}$	Δ	$U_{\bar{K}}(n_0)$	CFL			u_{cent}	$\frac{M_{max}}{M_{solar}}$
				u_l	u_u	$u_{th}^{K^-}$		
	(MeV)	(MeV)	(MeV)					
npΛΞ→ CFL+K^0	180	30		3.14	4.43		4.07	1.578
	180	57		2.27	3.97		3.97	1.477
	182	57		2.60	4.20		4.06	1.530
	184	57		3.02	4.48		4.06	1.569
npK^-→ CFL+K^0	180	30	-180	3.05	4.48	2.18	4.21	1.598
	180	57	-180	2.14	3.97	2.36	3.82	1.503
npΛΞK^-→ CFL+K^0	180	30	-180	4.73	5.19	2.29	4.87	1.497
	180	57	-180	2.27	3.94	2.68	3.82	1.464
	185	57	-160	3.28	4.63	3.20	4.27	1.582

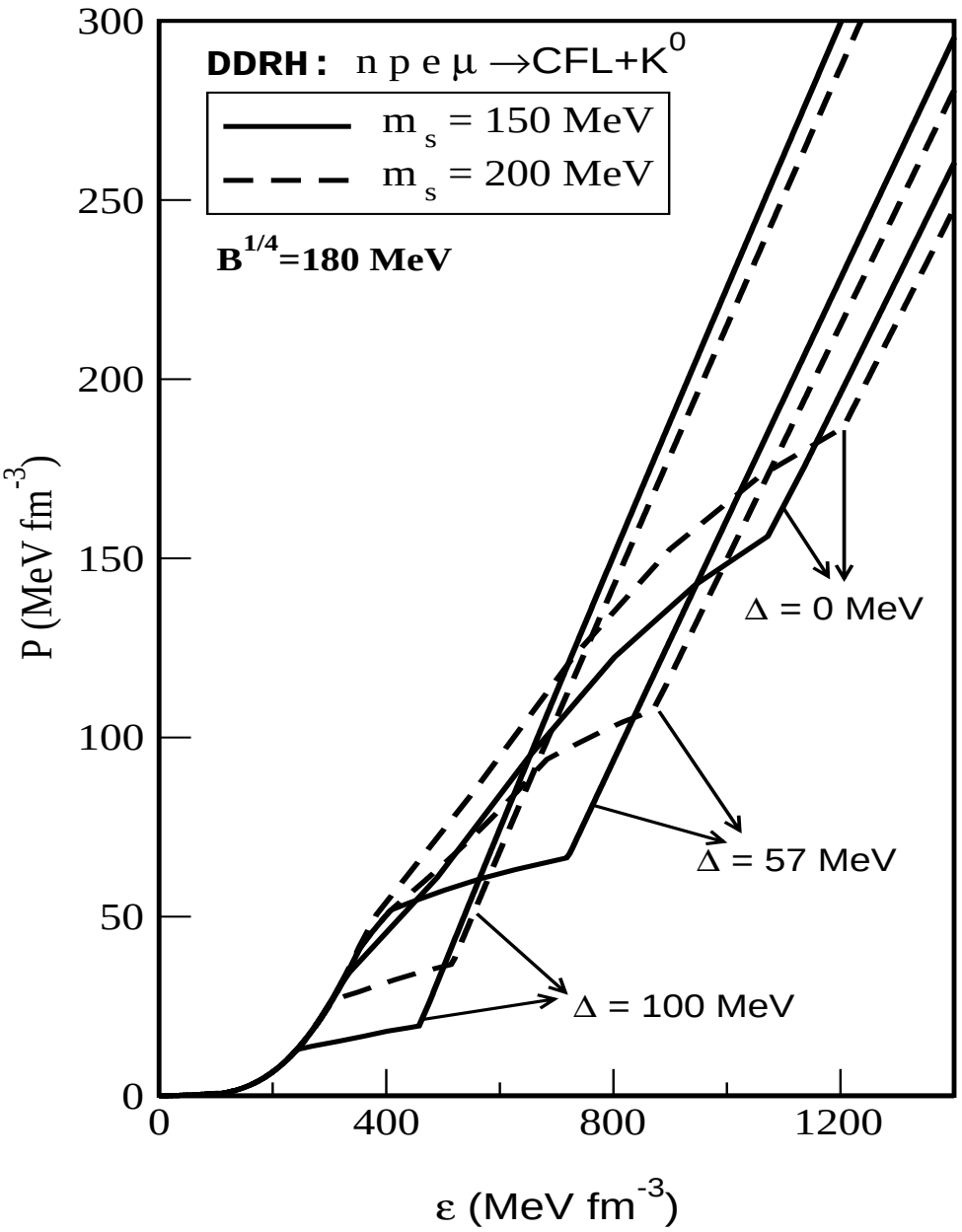

FIG. 1. The equations of state, pressure P versus energy density ε for n, p, lepton and CFL quark matter including K^0 condensate with $B^{1/4} = 180$ MeV and different values of Δ=0 (unpaired quark matter), 57 MeV and 100 MeV and m_s= 150 MeV and 200 MeV are compared.

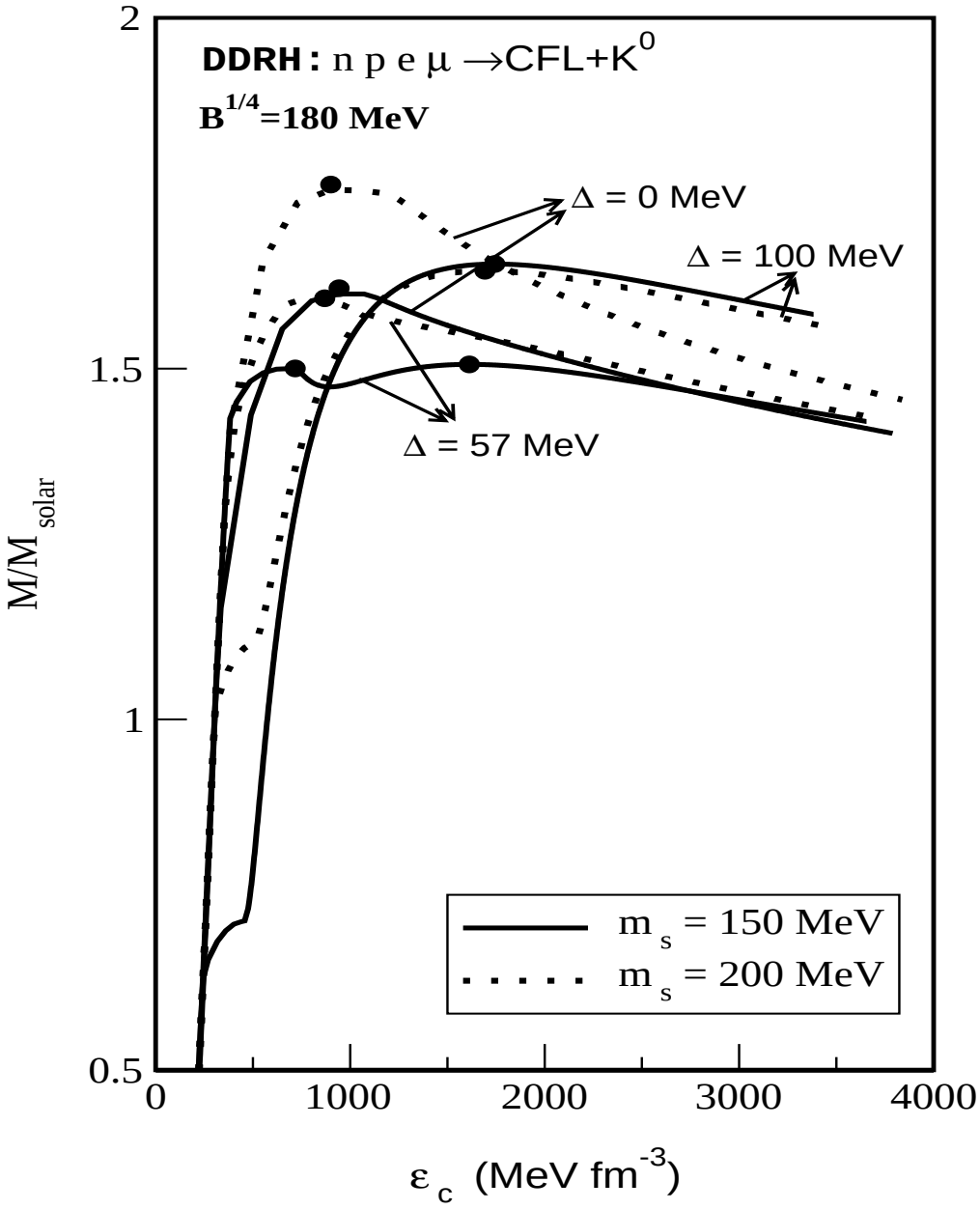

FIG. 2. The corresponding mass sequences for EoS of Fig. 1 are plotted .

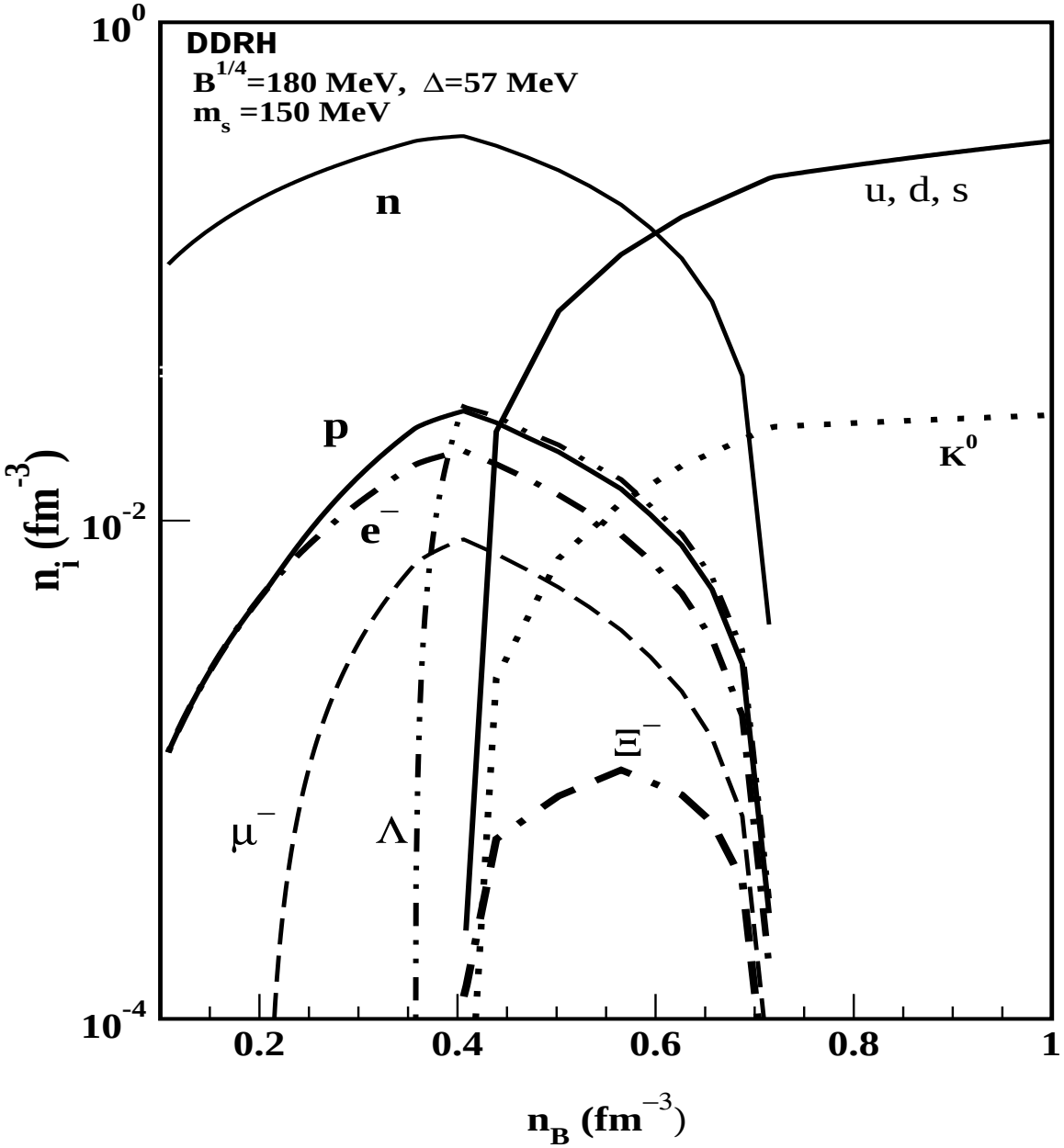

FIG. 3. Number densities (n_i) of various particles in β-equilibrated n, p, Λ, Ξ, lepton and CFL+K^0 matter for $B^{1/4}$ = 180 MeV, Δ= 57 MeV, and m_s= 150 MeV as a function of baryon density.

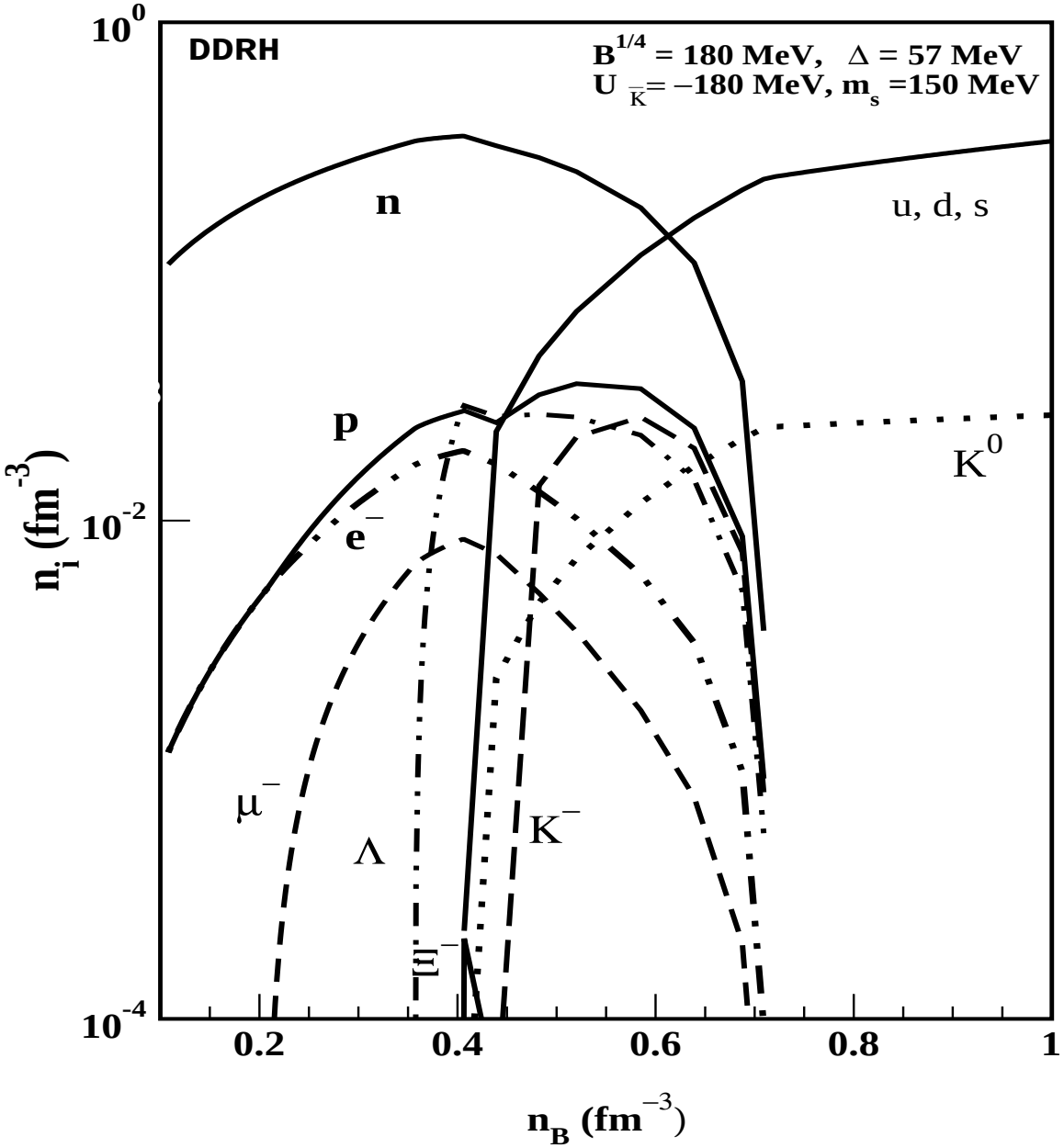

FIG. 4. Number densities (n_i) of various particles in β-equilibrated n, p, Λ, Ξ, K^-, lepton and CFL+K^0 matter for $B^{1/4} = 180$ MeV, Δ= 57 MeV, m_s= 150 MeV and antikaon optical potential depth $U_{\bar{K}}(n_0) = -180$ MeV at normal nuclear matter density as a function of baryon density .

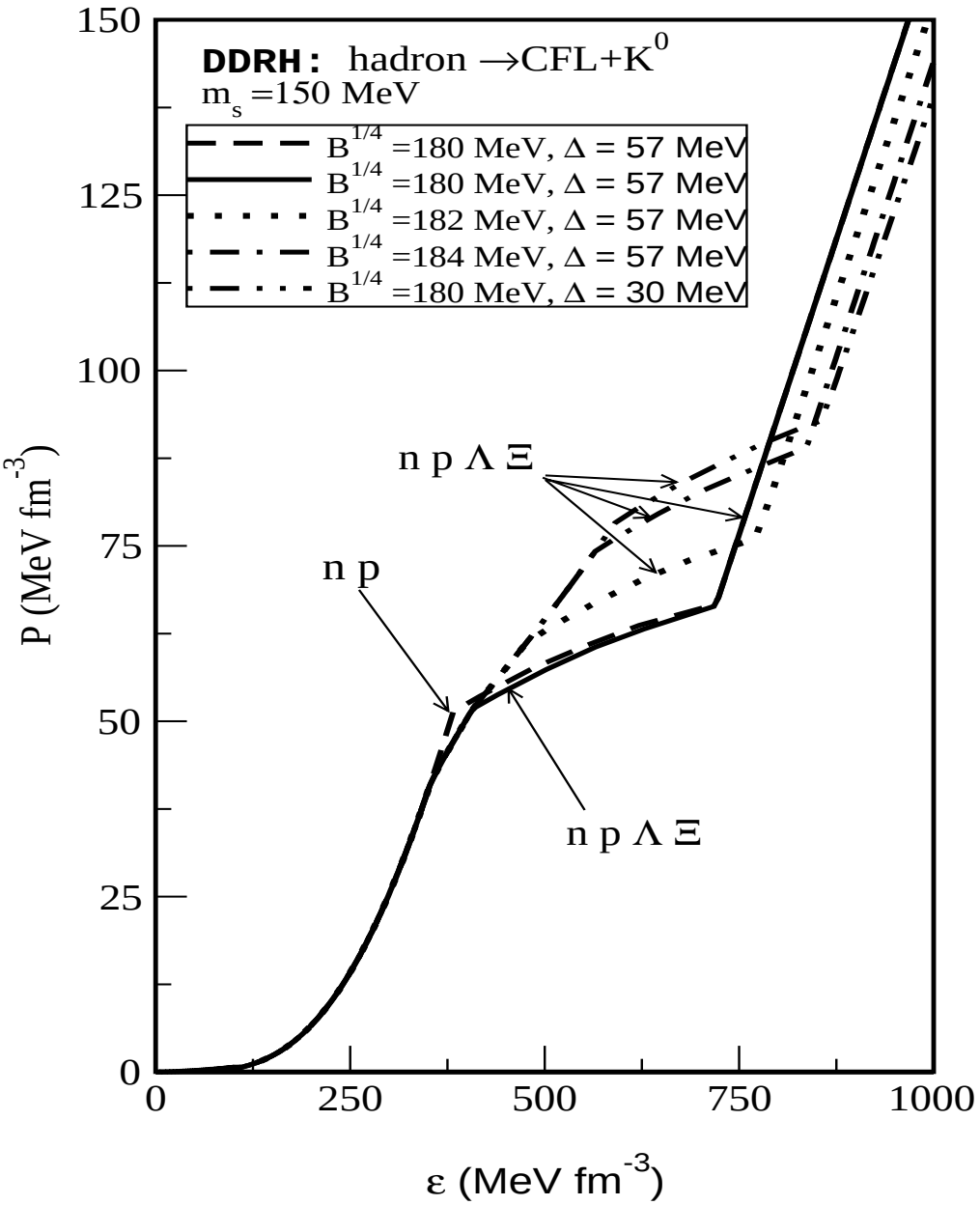

FIG. 5. The equation of state, pressure P versus energy density ε is shown here. The results are for n, p, lepton and CFL+K^0 matter (dashed line) and n, p, Λ, Ξ, lepton and CFL+K^0 matter (other lines) for m_s= 150 MeV and different values of bag constant and gap.

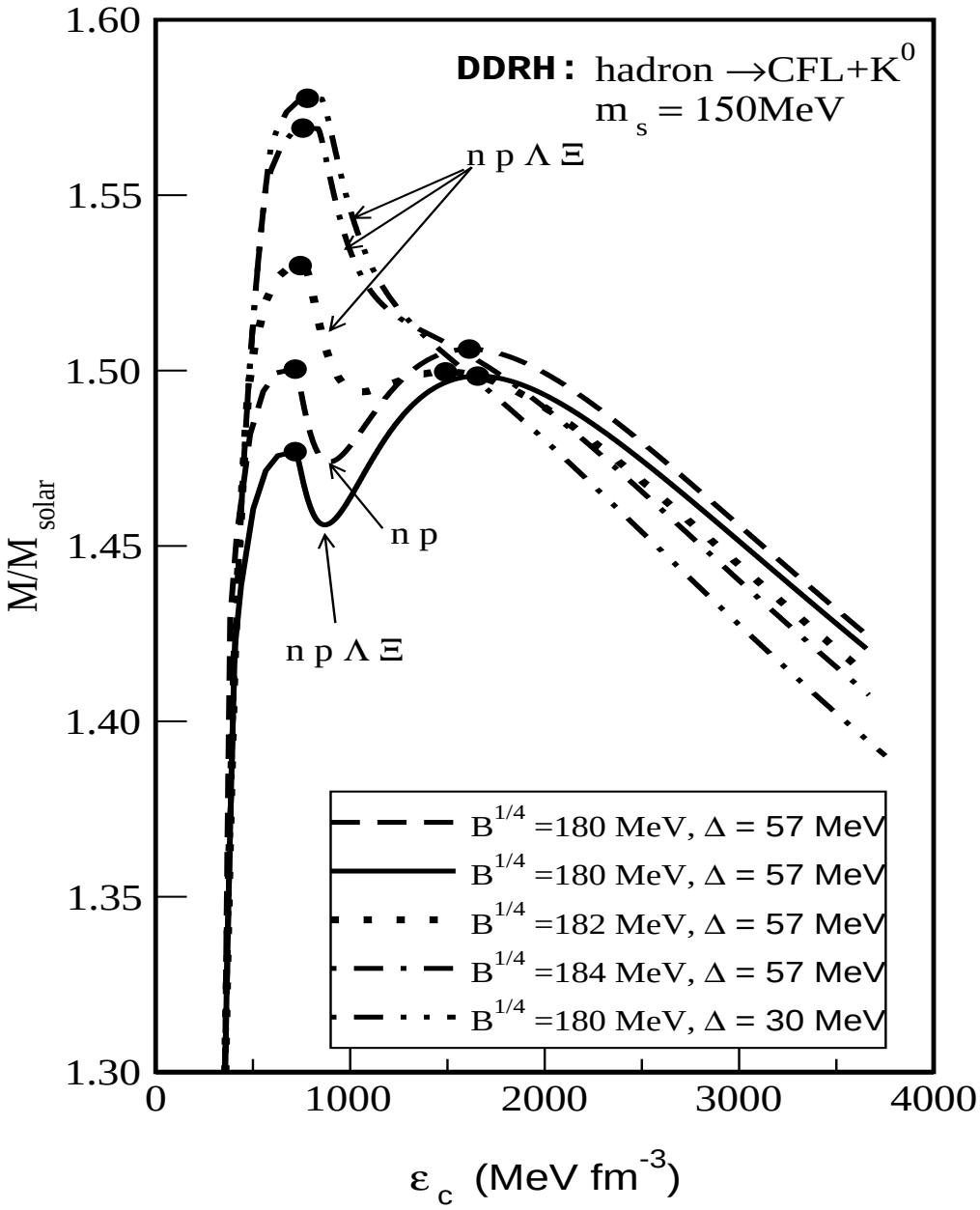

FIG. 6. The compact star mass sequences are plotted with central energy density for the corresponding EoS of Fig. 5.

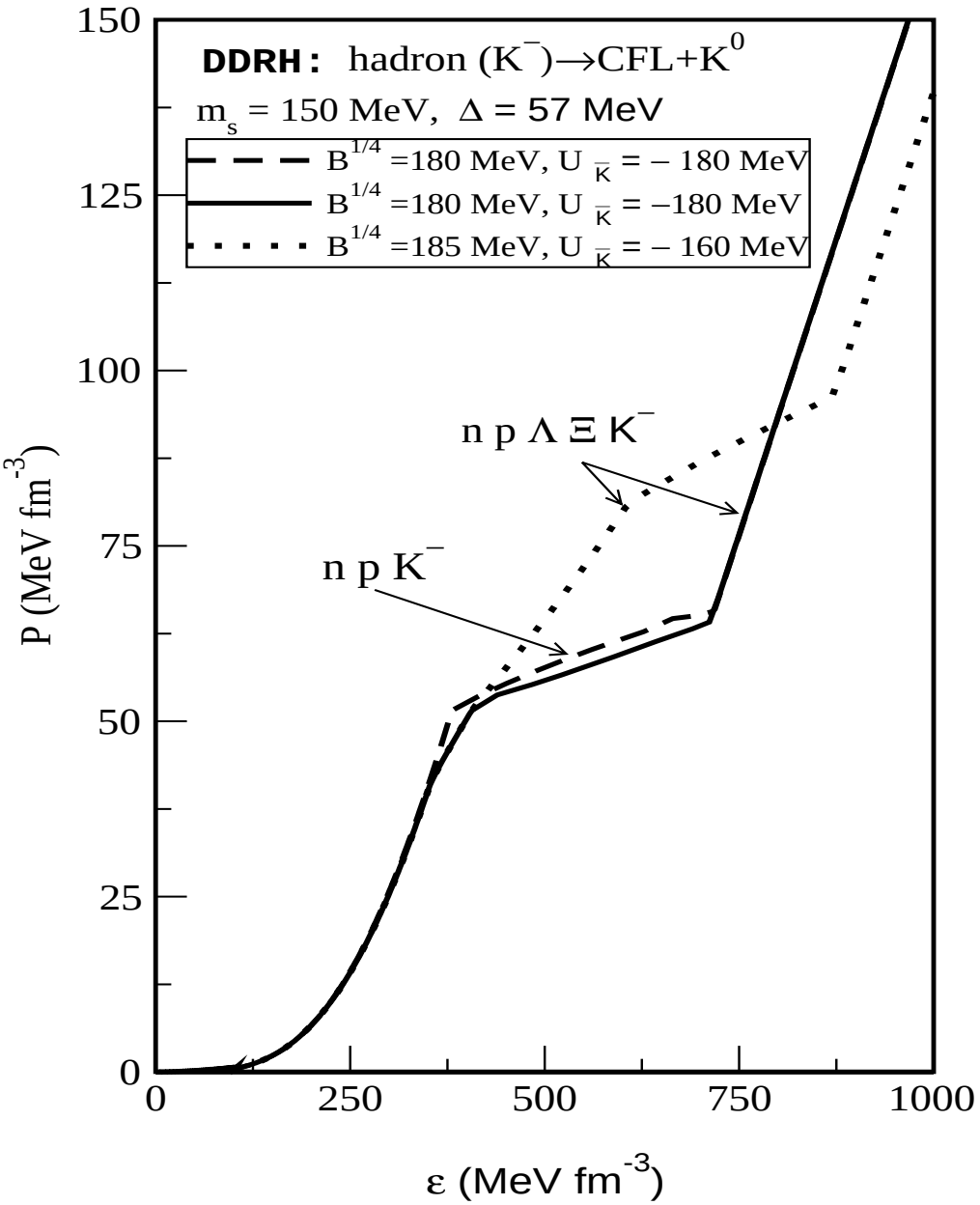

FIG. 7. The equation of state, pressure P versus energy density ε, is shown here. The results are for hadronic matter including K^- condensate and CFL+K^0 matter for m_s= 150 MeV, Δ=57 MeV and different values of bag constant and antikaon optical potential depth $U_{\bar{K}}(n_0) = -160$ and -180 MeV at normal nuclear matter density.

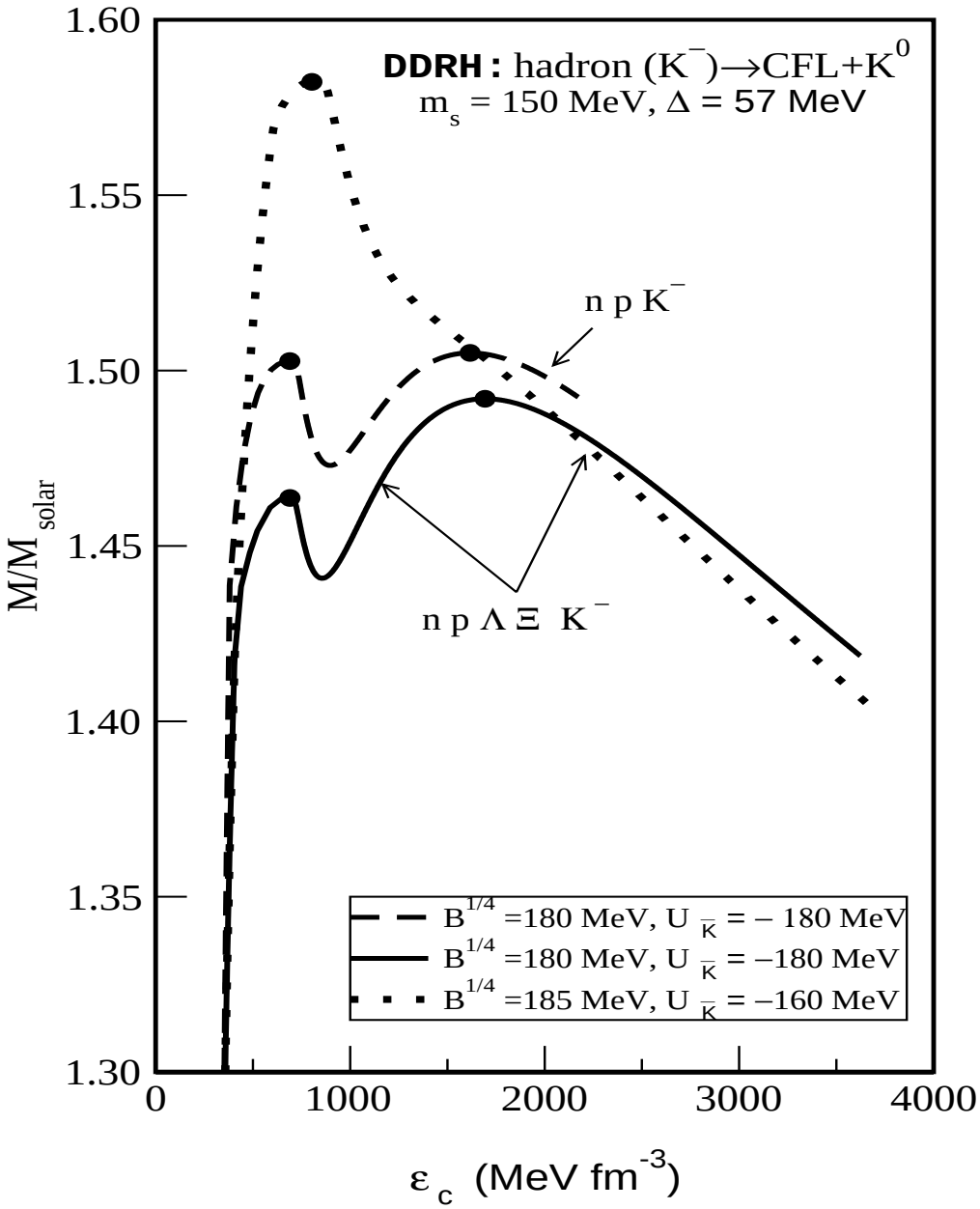

FIG. 8. The compact star mass sequences are plotted with central energy density for the corresponding EoS of Fig. 7.

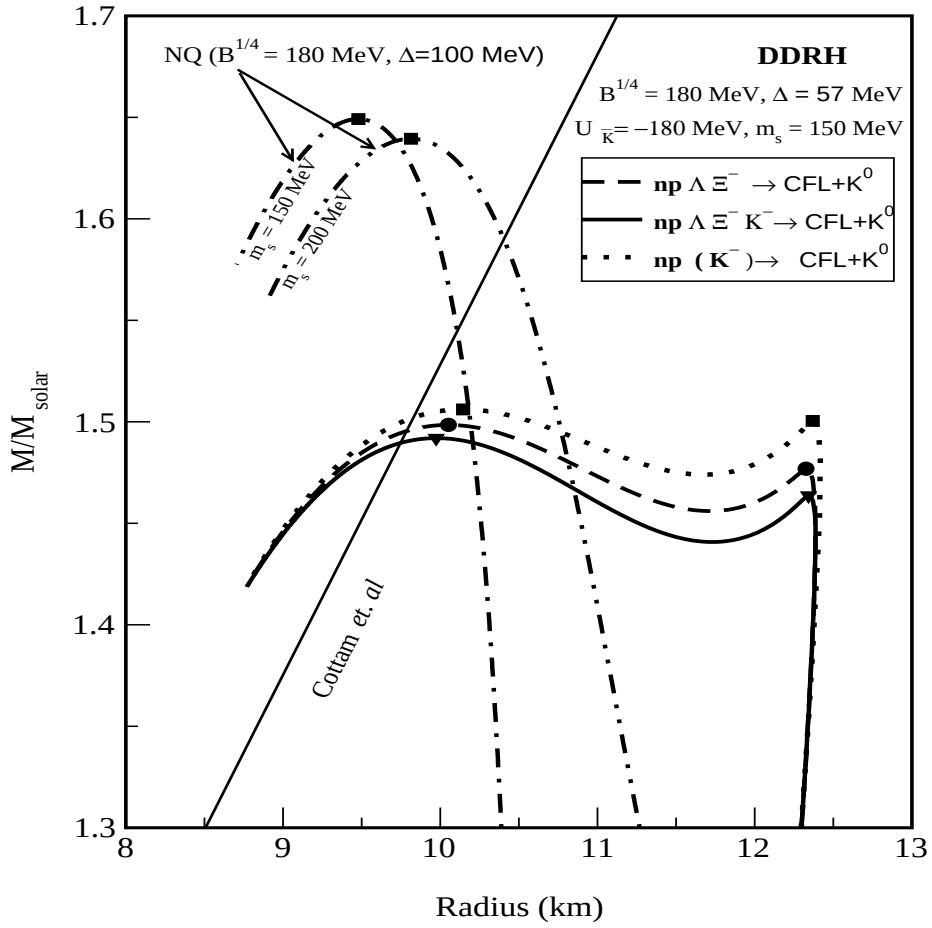

FIG. 9. The mass-radius relationship for compact star sequences for n, p, Λ, Ξ, lepton and CFL+K^0 matter with $B^{1/4}$ = 180 MeV, m_s= 150 MeV, Δ = 57 MeV and with K^- ($U_{\bar{K}}(n_0) = -180$ MeV) and without K^- condensate. Also, the results for NQ stars with $\Delta = 100$ MeV and different values of m_s are shown here.